PtTe Monolayer: Two-Dimensional Electrocatalyst with High Basal Plane Activity toward Oxygen Reduction Reaction

Wang, Y.; Li, Y.; Heine, T.;

Originally published:

October 2018

Journal of the American Chemical Society 140(2018)40, 12732-12735

DOI: https://doi.org/10.1021/jacs.8b08682

PtTe Monolayer: Two-dimensional Electrocatalyst with High Basal Plane Activity towards Oxygen Reduction Reaction

Journal:	*Journal of the American Chemical Society*
Manuscript ID	ja-2018-08682a.R1
Manuscript Type:	Communication
Date Submitted by the Author:	13-Sep-2018
Complete List of Authors:	Wang, Yu; Nanjing Normal University, Chemistry and Materials Science Li, Yafei; Nanjing Normal University - Xianlin Campus, School of Chemistry and Materials Science Heine, Thomas; TU Dresden, School of Science; Helmholtz Center Dresden-Rossendorf, Leipzig Branch, Institute of Resource Ecology

PtTe Monolayer: Two-dimensional Electrocatalyst with High Basal Plane Activity towards Oxygen Reduction Reaction

Yu Wang,[†] Yafei Li,*[,†] and Thomas Heine*[,‡,§]

[†]Jiangsu Collaborative Innovation Centre of Biomedical Functional Materials, Jiangsu Key Laboratory of New Power Batteries, School of Chemistry and Materials Science, Nanjing Normal University, Nanjing 210023, China.

[‡] TU Dresden, School of Science, Theoretical Chemistry, Bergstraße 66c, 01062 Dresden, Germany.

[§] Helmholtz-Zentrum Dresden-Rossendorf, Forschungsstelle Leipzig, Permoserstraße 15, 04318 Leipzig, Germany

Supporting Information Placeholder

ABSTRACT: PtTe is a layered bulk material that has been discovered in 1897. According to first principles calculations, it is one of the few layered materials that maintains structure and metallic character when thinned down to the monolayer. Interlayer energy is small enough to allow for chemical exfoliation techniques. Our calculations show that monolayer PtTe is a candidate to substitute Pt electrodes, and we computationally studied the catalytic performance of the oxygen reduction reaction (ORR). Remarkably, the basal plane of PtTe monolayer exhibits excellent catalytic activity towards ORR with a positive half-wave potential (~0.90 V) and a high four-electron (4e) reduction pathway selectivity. These characteristics suggest that it outperforms the catalytic performance of Pt electrodes, has a reduced Pt content, high Pt utilization and a high surface area, and make it a promising candidate for fuel cell components.

Fuel cells, which directly convert chemical energy into electricity through an electrochemical reaction, are one of the most promising solutions for future energy supply. Normally, the kinetics of cathode oxygen reduction reaction (ORR) in fuel cells is much slower than the anode reaction, which makes it the bottleneck for the overall fuel cell performance.[1] A catalyst is required to speed up the ORR kinetics, which is dominated, at the current stage, by platinum (Pt)-based materials. Though some non-Pt and even metal free catalysts have been proposed in recent years,[2] their catalytic performance and long-term durability are still overshadowed by Pt-based catalysts. The high price of Pt-based catalysts significantly hinders their large-scale commercialization. To achieve sustainable development of fuel cells, it is crucial to reduce the Pt-loading in Pt-based catalysts without sacrificing the catalytic activity, which thus requires a high utilization of Pt atoms.

In recent years, the rise of two-dimensional (2D) materials has brought new opportunities for the development of efficient catalysts.[3] Compared with traditional materials, 2D materials have high specific surface area and surface atomic ratio, which are very beneficial to their application in the field of catalysis. Inspired by the extensive studies of 2D materials, many groups have reported the synthesis of 2D ultrathin Pt-containing nanosheets and even monolayer, which exhibit excellent ORR catalytic activity in comparison to commercial Pt/C catalysts.[4] However, these 2D Pt-containing catalysts are mostly supported on other noble metals (e. g. Au, Pd) rather than the free-standing or dispersed genuine 2D structures, which is not favorable for efficient catalysis. In the 1950s, Grønvold et al. demonstrated that Pt also can bind with chalcogenide elements (S, Se, Te) to form layered dichalcogenides.[5] After exfoliation has been proposed,[6] many Pt-containing chalcogenides (e. g. PtS_2[7], $PtSe_2$[8]) have been synthesized. Unfortunately, these 2D Pt-containing dichalcogenides were all identified to be semiconducting without electronic states at the Fermi level,[6-9] and thus are intrinsically inert to ORR. Therefore, at present, free-standing Pt-containing 2D metals with excellent ORR catalytic activity are still not known.

In this paper, we propose an intriguing 2D Pt-containing material as ORR catalyst, namely PtTe monolayer, on the basis of comprehensive density functional theory (DFT) calculations (see SI for the computational details). It is found that PtTe monolayer is experimentally feasible, with high mechanical, thermodynamic and chemical stability. Different from semiconducting 2D Pt-containing dichalcogenides, PtTe monolayer is metallic due to the existence of an inner metallic Pt layer. Remarkably, the basal plane of PtTe monolayer exhibits superior catalytic activity and high four-electron (4e) selectivity towards electrochemical ORR, endowing it for promising applications in fuel cells.

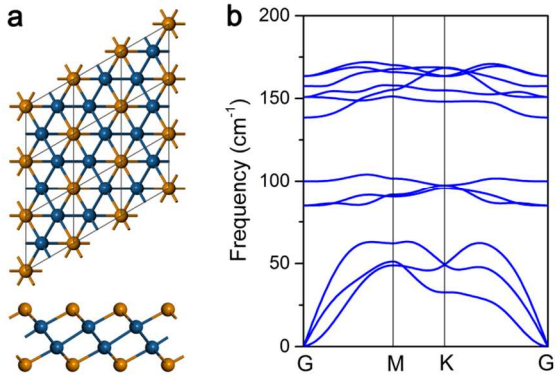

Figure 1. (a) Top (upper) and side (bottom) views of geometric structure, and (b) phonon spectrum of PtTe monolayer. Blue and orange balls represent Pt and Te atoms, respectively.

Bulk PtTe has been known since 1897[10] while its layered structure was determined by Bhan and co-workers in 1969.[11] **Figure S1** depicts the geometric structure of bulk PtTe, which can be regarded as the *ABC* stacking of PtTe layers in space group $R\bar{3}m$. The lattice parameters of bulk PtTe were optimized to be $a = b =$

3.95 Å, c = 19.86 Å at PBE-D3 level of theory, which agree well with Bhat et al.'s experimental data (a = b = 3.96 Å, c = 19.98 Å).[11] Each PtTe monolayer comprises two Pt atomic layers sandwiched between two Te atomic layers (**Figure 1a**). To evaluate the experimental feasibility of PtTe monolayer, we computed the cleavage energy (E_{cl}) of PtTe monolayer by introducing a fracture in a five-layers slab model of PtTe (**Figure S2**). The determined E_{cl} of PtTe (0.95 J m^{-2}) is comparable to some recently exfoliated 2D structures, such as MoS_2 (0.42 J m^{-2})[12] and Ca_2N (1.09 J m^{-2})[13], suggesting that isolation of 2D PtTe monolayer from the bulk is feasible via exfoliation strategies.

The lattice constants of PtTe monolayer were optimized to be a = b = 3.99 Å, which are slightly larger than those of bulk PtTe. It has a diamagnetic ground state, indicating that there are no unpaired electrons or dangling bonds in PtTe monolayer. The kinetical stability of PtTe monolayer is confirmed by its phonon dispersion (**Figure 1b**), where no imaginary phonon branches can be found. The elastic constants of PtTe monolayer (C_{11} = C_{22} = 73.66 N/m, C_{12} = 35.60 N/m, and C_{66} = 19.03 N/m) meet the criteria for a hexagonal 2D crystal (C_{11} > $|C_{12}|$, C_{66} >0), indicating that it is mechanically stable. Moreover, first-principles molecular dynamics (FPMD) simulations (4×4 supercell) demonstrate that the structure of PtTe monolayer remains intact throughout the 10 ps FPMD up to 1200 K (**Figure S3a**), indicating that PtTe monolayer is thermodynamically stable. Encouragingly, there is no spontaneous dissociation for O_2 molecule on the surface of PtTe monolayer after a 10 ps FPMD simulation at 300 K, implying that PtTe monolayer would not prone to oxidation and is stable at ambient conditions (**Figure S3b**).

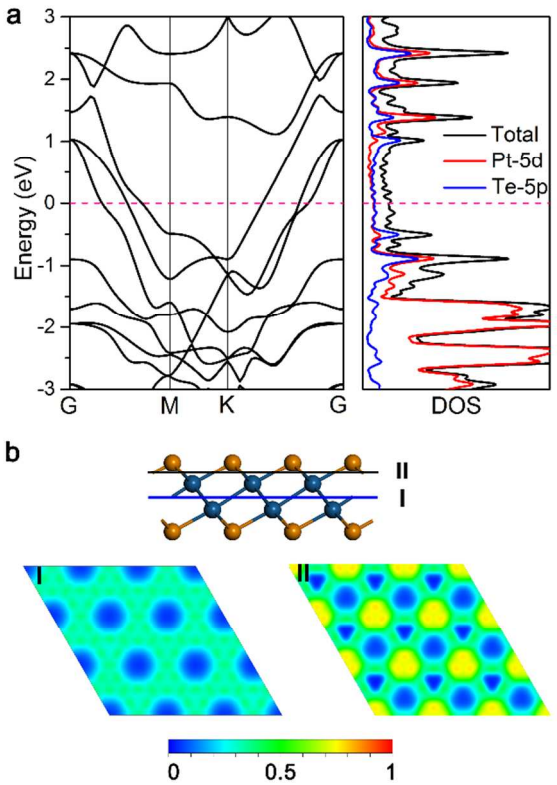

Figure 2. (a) Band structure (left) and density of states (DOS) (right) of PtTe monolayer. (b) Sliced electron localization function (ELF) of PtTe monolayer along the (001) plane. I and II label two sliced planes through the center of Pt-Pt and Pt-Te bonds, respectively. The iso-values of 0 and 1 imply low and high electron localization, respectively.

After confirming the stability of PtTe monolayer, we next explored its electronic properties. As shown in **Figure 2a**, PtTe monolayer maintains the metallic character of its bulk counterpart (**Figure S4**). Here we re-computed the band structure using HSE06 functional (**Figure S5**),[14] which also predicted a metallic nature for PtTe monolayer. The analysis of partial density of states (PDOS) reveals that the states near the Fermi level are contributed by both Pt-5d and Te-5p states, which can be confirmed by the partial charge density in energy range of –0.5 to 0 eV vs. Fermi level (**Figure S6**). The electron localization function (ELF), shown in **Figure 2b** for the (001) plane sliced through the center plane (inbetween the Pt atoms), reveals a typical electron-gas-like metallic picture with an ELF iso-value of around 0.4. Moreover, the ELF iso-value of Pt−Te bond center is around 0.5, indicative of delocalized bonding character. Therefore, both atom types contribute almost equally to the metallic character of PtTe monolayer.

The aforementioned results demonstrate that PtTe monolayer is a metallic material which is expected to be obtained by exfoliation experiments from the bulk. We are quite curious whether this novel 2D structure is a promising candidate for fuel cell applications as other Pt-based nanomaterials have displayed outstanding performance for launching the sluggish ORR. To this end, we then explored the ORR catalytic activity of PtTe monolayer on the basis of the computational hydrogen electrode (CHE) model.[15]

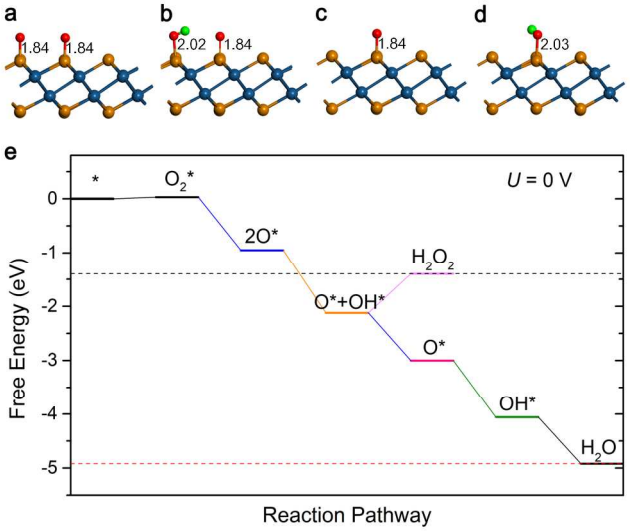

Figure 3. Geometrics of ORR intermediates: (a) 2O*, (b) O*+OH*, (c) O*, and (d) OH*. The red and green balls represent O and H atoms, respectively. e) Free energy diagrams for the dissociative ORR pathway on PtTe basal plane at U = 0 V. The Te-O bond lengths are given in Å.

Generally, there are two reaction mechanisms for ORR, namely the dissociative (**equation S(1)**) and the associative (**equation S(2)**) ones. The first step is the adsorption of O_2 on PtTe monolayer, where, intriguingly, the outer Te atoms of PtTe monolayer were found to be the active sites for O_2 activation rather than the inner Pt atoms, which is different from previously reported Pt-containing ORR catalysts. When O_2 reaches the surface of PtTe monolayer, the O−O bond length is significantly stretched from 1.23 Å to be 1.35 Å, indicating that O_2 has been effectively activated. Moreover, the activated O_2 molecule, which has been tuned from triplet into singlet, can be dissociated into two adsorbed O* species with a small energy barrier of 0.32 eV (**Figure S7**), which is lower than the O_2 dissociation barrier of O_2 on Pt (111) (0.48 eV)[16]. Therefore, we mainly focused on the dissociative mechanism as it appears to be the most like reduction pathway. The

atomic configurations of ORR intermediates along the reaction path are displayed in **Figure 3a-3d**.

From the free energy diagram, one can see that all the electrochemical steps are downhill at U = 0 V (**Figure 3e**), and the protonation of OH* to H_2O is the potential-limiting step for the whole ORR process with a ΔG of −0.86 eV. Therefore, the maximum value of U at which all reactions are still exothermic (namely limiting-potential, for details see SI) is accordingly predicted to 0.86 V for PtTe monolayer (**Figure S8**), which is even higher than that of Pt (111) (0.79 V),[16,17] suggesting that PtTe monolayer has a rather good ORR activity. As suggested by Nørskov et al.,[18] the ΔG of OH* to H_2O for an ideal ORR catalyst is also −0.86 eV, which implies that PtTe monolayer has actually reached the top of 4e ORR activity volcano.

In addition to superior activity, PtTe monolayer exhibits a high selectivity for four-electron (4e) reduction pathway. As shown in **Figure 3e** and **Figure S8**, the H_2O_2 formation step is extremely endothermic, suggesting that the two-electron (2e) pathway could be significantly suppressed by the 4e pathway under the normal working conditions. Therefore, PtTe monolayer can act as a promising low-Pt catalyst in fuel cells as it has high activity and selectivity towards ORR as well as has a high density of active sites (~1.45×10^{15}/cm^2).

To give an intuitive demonstration of the superior ORR catalytic performance for PtTe monolayer, we simulated its polarization curve and compared to that of Pt by means of micro-kinetic simulations. As shown in **Figure 4**, the predicted onset potential (at j = 50 μA cm^{-2}) of PtTe monolayer is ~0.93 V vs. RHE, and the half-wave potential reaches ~0.90 V *vs.* RHE, which outperforms Pt (111) by ~50 mV. Therefore, PtTe monolayer is expected to show better ORR catalytic activity than Pt and it could be a promising alternative to the state-of-the art commercial Pt electrodes.

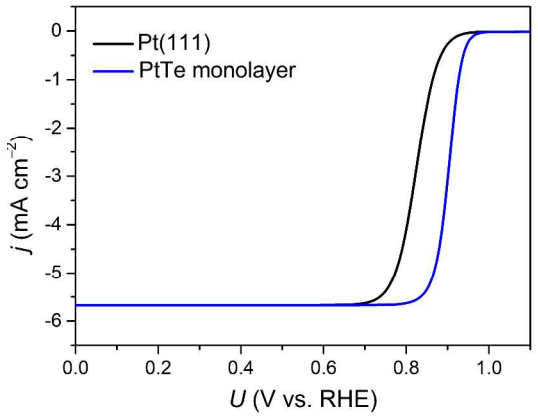

Figure 4. Simulated polarization curves of PtTe monolayer and Pt (111). The energy data of Pt (111) are taken from refs. 16 and 17.

The high basal plane activity of PtTe monolayer can be understood from its unique charge distribution. According to the Bader charge population analysis, there is a significant charge transfer from the outer Te atoms to the inner Pt atoms, resulting in a net charge of −0.39 and 0.39 |e| for Pt and Te, respectively. The positively charged Te sites can provide an empty p-orbital to active O_2 molecular and then trigger the whole ORR process. This electron activation mechanism is similar to that known for N doped carbon materials, where the active sites are positively charged carbon atoms neighboring to the nitrogen dopant.[19] Moreover, we plot the partial DOS of the intermediates to get some vivid insights. As shown in **Figure S9**, there are obvious hybridizations between the 2p orbitals of the adsorbed species and the Te site-5p orbital.

Considering that the adsorbed O_2* might be directly protonated to form OOH* before dissociating into O* species, we also studied the association ORR mechanism of PtTe monolayer and identified a high limiting-potential of 0.85 V (**Figure S10**), which is quite close to that of the dissociative mechanism. Interestingly, it is found that the basal plane of thicker PtTe nanosheet (**Figure 11**) can maintain the excellent ORR activity as that identified for monolayer. In contrast, the edge sites of PtTe monolayer are actually inert to ORR due to the too strong interaction between edge atoms and OH* intermediate (**Figure S12**).

In summary, we systematically studied the structural, electronic, and catalytic properties of a novel 2D material, namely PtTe monolayer, on the basis of comprehensive DFT calculations. According to our results, PtTe monolayer is a stable 2D structure and can be obtained probably via exfoliation method. Due to the presence of inner Pt layer, PtTe monolayer is metallic with considerable electronic states at the Fermi level. In particular, the CHE model-based computations demonstrated that PtTe monolayer is a promising ORR catalyst candidate with an outstanding catalytic activity and a high 4e reduction pathway selectivity. Due to the high experimental feasibility and structural stability, it is expected that PtTe monolayer could be realized in the lab and be utilized as ORR catalyst in the near future. We also hope our studies would motivate experimental and theoretical efforts on developing more 2D Pt-based ORR catalysts.

ASSOCIATED CONTENT

Supporting Information

The Supporting Information is available free of charge via the Internet at http://pubs.acs.org.
Computational methods, structure of bulk PtTe, cleavage energy estimation, MD simulations results, band structure of bulk PtTe, HSE06 band structure of PtTe monolayer, partial charge density, energy barrier of O_2 dissociation, O_2 dissociative pathway at 0.86 V, PDOS of ORR intermediates, free energy diagram for associative pathway, free energy diagram and corresponding structures for ORR proceeded on the basal plane of PtTe trilayer and edge sites of PtTe monolayer.

AUTHOR INFORMATION

Corresponding Author

*liyafei@njnu.edu.cn
*thomas.heine@tu-dresden.de

Notes

The authors declare no competing financial interests.

ACKNOWLEDGMENT

We are grateful for funding support from the Natural Science Foundation of China (No. 21522305), the NSF of Jiangsu Province of China (No. BK20150045), and the Priority Academic Program Development of Jiangsu Higher Education Institutions. TH thanks Deutsche Forschungsgemeinschaft (Grant HE 3543/27-1).

REFERENCES

(1) (a) Debe, M. K. *Nature* **2012**, *486*, 43. (b) Steele, B. C. H.; Heinzel, A. *Nature*, **2001**, *414*, 345.
(2) (a) Wu, J.; Yang, H. *Acc. Chem. Res.* **2013**, *46*, 1848. (b) Lin, R.; Cai, X.; Zeng, H.; Yu, Z. *Adv. Mater.* **2018**, *30*, 1705332. (c) Bing, Y.; Liu, H.; Zhang, L.; Ghosh, D.; Zhang, J. *Chem. Soc. Rev.* **2010**, *39*, 2184. (d) Sui, S.; Wang, X.; Zhou, X.; Su, Y.; Riffat, S.; Liu, C. J. *J. Mater. Chem. A* **2017**, *5*, 1808. (e) Huang, X. Q.; Zhao, Z. P.; Cao, L.; Chen, Y.; Zhu, E. B.; Lin, Z. Y.; Li, M. F.; Yan, A. M.; Zettl, A.; Wang, Y. M.; Duan, X. F.;

Mueller, T.; Huang, Y. *Science* **2015**, *348*, 1230. (f) Huang, H.; Li, K.; Chen, Z.; Luo, L.; Gu, Y.; Zhang, D.; Ma, C.; Si, R.; Yang, J.; Peng, Z.; Zeng, J. *J. Am. Chem. Soc.* **2017**, *139*, 8152. (g) Zhong, H. X.; Wang, J.; Zhang, Y. W.; Xu, W. L.; Xing, W.; Xu, D.; Zhang, Y. F.; Zhang, X. B. *Angew. Chem. Int. Ed.* **2014**, *53*, 14235.
(3) Deng, H.; Novoselov, K. S.; Fu, Q.; Zheng, N.; Tian, Z.; Bao, X. *Nat. Nanotechnol.* **2016**, *11*, 218.
(4) (a) Zhang, J.; Vukmirovic, M. B.; Xu, Y.; Mavrikakis, M.; Adzic, R. R. *Angew. Chem. Int. Ed.* **2005**, *44*, 2132. (b) Sasaki, K.; Wang, J. X.; Naohara, H.; Marinkovic, N.; More, K.; Inada, H.; Adzic, R. R. *Electrochim. Acta.* **2010**, *55*, 2645. (c) Cai, B.; Hübner, R.; Sasaki, K.; Zhang, Y.; Su, D.; Ziegler, C.; Vukmirovic, M. B.; Rellinghaus, B. Adzic, R. R.; Eychmüller, A. *Angew. Chem. Int. Ed.* **2018**, *57*, 2963. (d) Tian, X.; Luo, J.; Nan, H.; Zou, H.; Chen, R.; Shu, T.; Li, X.; Li, Y.; Song, H.; Liao, S.; Adzic, R. R. J. Am. Chem. Soc. 2016, 138, 1575. (e) Bu, L.; Zhang, N.; Guo, S.; Zhang, X.; Li, J.; Yao, J.; Wu, T.; Lu, G.; Ma, J. Y.; Su, D.; Huang, X. *Science* **2016**, *354*, 1410
(5) (a) Grønvold, F.; Rost, E. *Acta Chem. Scand.* **1956**, *10*, 1620. (b) Kjekshus, A.; Grønvold, F. *Acta Chem. Scand.* **1959**, *13*, 1767. (c) Grønvold, F.; Haraldsen, H.; Kjekshus, A. *Acta Chem. Scand.* **1960**, *14*, 1879.
(6) Miró, P.; Ghorbani-Asl, M.; Heine, T. *Angew. Chem. Int. Ed.* **2014**, *53*, 3015.
(7) (a) Zhao, Y.; Qiao, J.; Yu, P.; Hu, Z.; Lin, Z.; Lau, S. P.; Liu, Z.; Ji, W.; Chai, Y. *Adv. Mater.* **2016**, *28*, 2399. (b) Li, L.; Wang, W.; Chai, Y.; Li, H.; Tian, M.; Zhai, T. *Adv. Funct. Mater.* **2017**, *27*, 1701011.
(8) (a) Wang, Y.; Li, L.; Yao, W.; Song, S.; Sun, J.; Pan, J.; Ren, X.; Li, C.; Okunishi, E.; Wang, Y.; Wang, E.; Shao, Y.; Zhang, Y.; Yang, H.; Schwier, E.; Iwasawa, H.; Shimada, K.; Taniguchi, M.; Cheng, Z.; Zhou, S.; Du, S.; Pennycook, S.; Pantelides, S.; Gao, H. J. *Nano Lett.* **2015**, *15*, 4013. (b) Wang, Z.; Li, Q.; Besenbacher, F.; Dong, M. *Adv. Mater.* **2016**, *28*, 10224.
(9) (a) Miró, P.; Audiffred, M.; Heine, T. *Chem. Soc. Rev.* **2014**, *43*, 6537. (b) Du, J.; Song, P.; Fang, L.; Wang, T.; Wei, Z.; Li, J.; Xia, C. *Appl. Sur. Sci.* **2018**, *435*, 476.
(10) Roessler, C. *Z. Anorg. Chem.* **1897**, *15*, 405.
(11) Bhan, S.; Godecke, T.; Schubert, K. *J. Less Common Metals* **1969**, *19*, 121.
(12) Björkman, T.; Gulans, A.; Krasheninnikov, A. V.; Nieminen, R. M. *Phys. Rev. Lett.* **2012**, *108*, 235502.
(13) Zhao, S.; Li, Z.; Yang, J. *J. Am. Chem. Soc.* **2014**, *136*, 13313.
(14) Heyd, J.; Scuseria, G. E.; Ernzerhof, M. *J. Chem. Phys.* **2003**, *118*, 8207.
(15) Nørskov, J. K.; Rossmeisl, J.; Logadottir, A.; Lindqvist, L.; Kitchin, J. R.; Bligaard, T.; Jónsson, H. *J. Phys. Chem. B* **2004**, *108*, 17886.
(16) Tripković, V.; Skúlason, E.; Siahrostami, S.; Nørskov, J. K.; Rossmeisl, J. *Electrochim. Acta* **2010**, *55*, 7975.
(17) (a) Karlberg, G. S.; Rossmeisl, J.; Nørskov, J. K. *Phys. Chem. Chem. Phys.* **2007**, *9*, 5158. (b) Hansen, H. A.; Viswanathan, V.; Nørskov, J. K. *J. Phys. Chem. C* **2014**, *118*, 6706.
(18) Viswanathan, V.; Hansen, H. A.; Rossmeisl, J.; Nørskov, J. K. *J. Phys. Chem. Lett.* **2012**, *3*, 2948.
(19) (a) Gong, K. P.; Du, F.; Xia, Z. H.; Durstock, M.; Dai, L. M. *Science* **2009**, *323*, 760. (b) Jiao, Y.; Zheng, Y.; Jaroniec, M.; Qiao, S. Z. *J. Am. Chem. Soc.* **2014**, *136*, 4394.

Table of Contents artwork